Chapter 9
Ion-Based Liquid Crystals: From Well-Defined Self-Organized Nanostructures to Applications

Hiromitsu Maeda

Abstract Recent progress in the chemistry of ion-based liquid crystals and related materials based on anion-responsive π-conjugated molecules is summarized. Thermotropic liquid crystals with highly ordered positively and negatively charged species are promising materials as organic semiconductors that show fascinating properties compared to those of electronically neutral species. The achievement of ion-based liquid crystals requires the preparation of appropriate charged building subunits, in particular, planar anionic species, which can be obtained by the complexation of electronically neutral anion-responsive π-conjugated molecules. The author's group has fabricated a variety of ion-based organized structures as liquid crystals comprising pyrrole-based anion receptor molecules. The charge-carrier transporting properties exhibited by some of the obtained materials highlight their potential utility in future applications.

9.1 Introduction

The geometries and substituents of organic molecules are very important factors that influence the formation of dimension-controlled organized structures [1–5]. The arrangement of appropriately designed molecules in ordered forms can facilitate the formation of soft materials [6], such as liquid crystals [7–12], which are extremely useful owing to their ability to change their bulk structures according to external conditions. π-Electronic molecules are promising building blocks of organized structures with their highly planar structures enabling efficient

H. Maeda (✉)
College of Pharmaceutical Sciences, Ritsumeikan University, Kusatsu 525-8577, Japan
e-mail: maedahir@ph.ritsumei.ac.jp

Q. Li (ed.), *Nanoscience with Liquid Crystals*, NanoScience and Technology,
DOI: 10.1007/978-3-319-04867-3_9,

stacking. In addition, they often exhibit optical absorption in the visible region, resulting in the ability to fabricate functional electronic materials. As one of the noncovalent interactions to afford molecular assemblies, the electrostatic interaction among charged species provides ion pairs both in solution and in the bulk states. Therefore, the geometries and electronic states of the ionic species are highly important for determining the properties of the ion pairs and their resulting assemblies. As is well known, bulky geometries in both the cationic and anionic components can produce ionic liquids by preventing crystallization through weakening of the ionic interactions [13–18], whereas carefully designed ionic species can provide dimension-controlled assemblies in the form of liquid crystals and related materials [8, 19–21]. However, most of the ion-based materials reported thus far have been fabricated using either cationic or anionic components as the main building blocks of the assemblies accompanied by the respective counter ions, or used electronically neutral components possessing charged moieties in their side chains. In order to effectively utilize the great potential of ion-based assemblies, a new strategy is required for fabricating the materials comprising both cations and anions as crucial building blocks.

The achievement of effectively stacking charged species requires planar geometries that can form dimension-controlled assemblies comprising cationic and anionic components in ordered arrangements. Appropriately designed planar charged species could provide a variety of assembly modes through the control of their interactions (Fig. 9.1). In this figure, a *charge-by-charge assembly* is defined as an organized structure comprising alternately stacking positively and negatively charged species, whereas a *charge-segregated assembly* results from the combination of the appropriate cations and anions and gives rise to electrostatic repulsion between species of the same charge. In the obtained materials, partial contributions from charge-by-charge and charge-segregated assemblies would be observed as an intermediate assembly mode. These ordered structures containing charged components (i.e. electron-deficient and electron-rich species) exhibit potential for use as organic semiconductors; in particular, charge-segregated assemblies may enable high charge-carrier densities by decreasing the electrostatic repulsion between identical charged species.

As compared to planar cations, it is not easy to synthesize planar anions for use as building blocks in stacking assemblies because of the excess electrons that encourage electrophilic attack on the anions. One promising strategy for preparing planar anionic structures is to combine electronically neutral planar anion-responsive molecules with inorganic anions such as halides, resulting in the formation of receptor–anion complexes as pseudo planar anions. Therefore, the design and synthesis of π-electronic systems with efficient anion-binding abilities would be extremely useful. Potential anion-responsive π-conjugated molecules [22–28] are dipyrrolyldiketone boron complexes (e.g. **1**–**3**, Fig. 9.2) [29–48], which show anion-binding behavior with inversion of the pyrrole rings to form planar receptor–anion complexes. Such anion receptors have been shown to be suitable motifs for fabricating assemblies and organized structures such as thermotropic liquid crystals in the anion-free form [35, 41, 44–46], owing to their

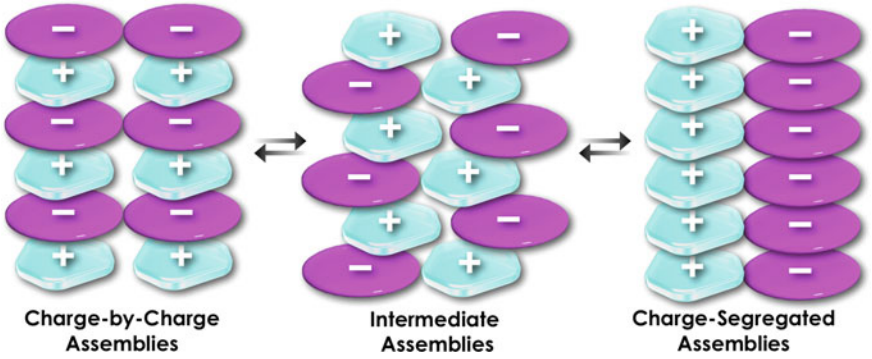

Fig. 9.1 Conceptual diagram of the assembly modes comprising charged species

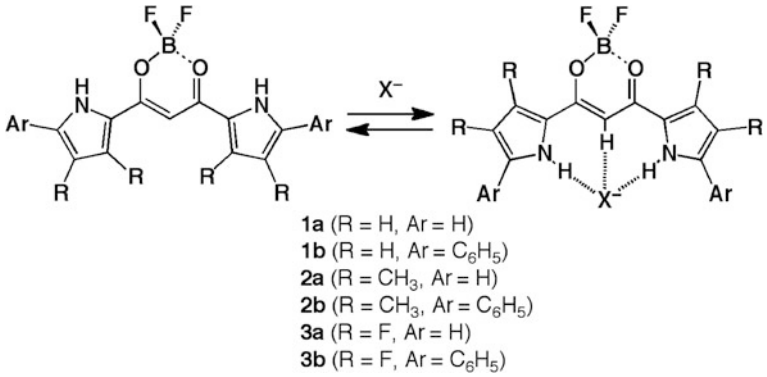

Fig. 9.2 Dipyrrolyldiketone BF_2 complexes and their anion-binding mode

fairly planar conformations and the ability to introduce various substituents that induce additional noncovalent interactions. Assemblies of such molecules exhibit anion-responsive behavior in the bulk state and fascinatingly, the formation of ion-pairing assemblies of the receptor–anion complexes and counter cations.

9.2 Solid-State Ion-Based Assembled Structures

The boron-1,3-propanedione moiety between the two pyrrole rings of the dipyrrolyldiketone boron complexes is effective in affording suitable electronic states that exhibit UV/vis absorption and emission maxima in the visible region, as observed at 432 and 451 nm, respectively, in CH_2Cl_2 for **1a** [32]. Upon the addition of anions as tetrabutylammonium (TBA^+) salts, interactions with the anions through the pyrrole NH and bridging CH can be identified by ^1H NMR chemical shifts, as has been examined for a series of anion receptors. UV/vis

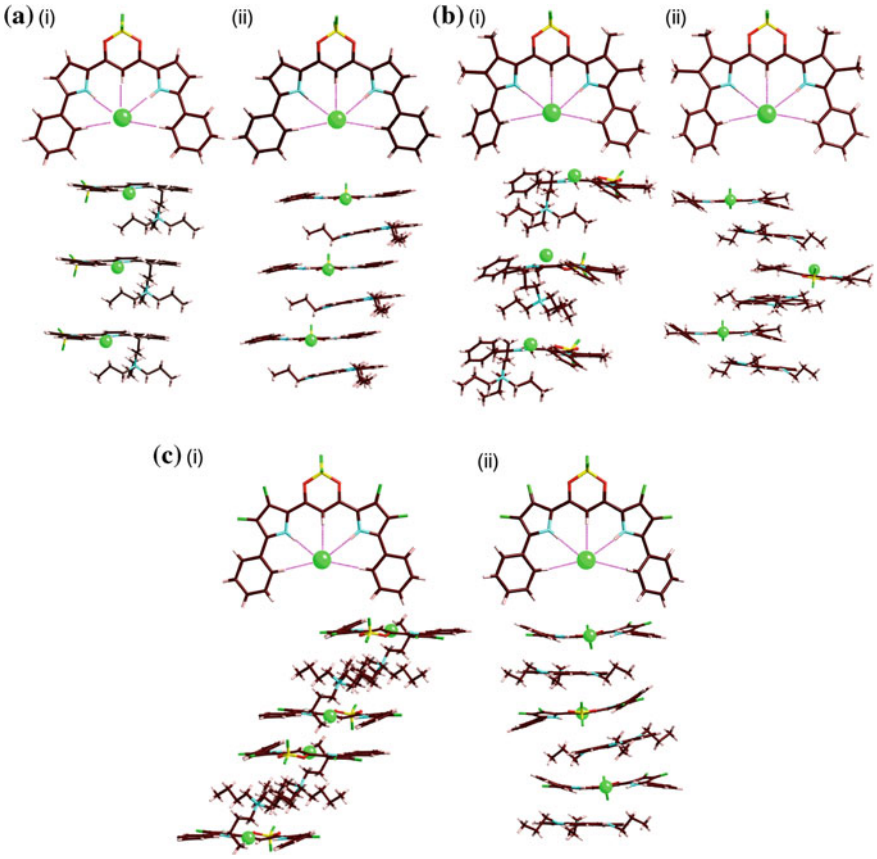

Fig. 9.3 Top and side-packing view from single-crystal X-ray analysis of **a***i* **1b**·Cl^--TPA^+ and *ii* **1b**·Cl^--$TATA^+$, **b***i* **2b**·Cl^--TPA^+ and *ii* **2b**·Cl^--$TATA^+$, and **c***i* **3b**·Cl^--TBA^+ and *ii* **3b**·Cl^--$TATA^+$ (reproduced from cif files: CCDC-646480, 781980, 78198, 745780, 853090, and 853091, respectively)

absorption and emission spectra of the anion receptors were also changed by anion binding, suggesting their potential as colorimetric and fluorescent sensors for anions. The anion-binding constants (K_a) of, for example, α-phenyl-substituted **1b** in CH_2Cl_2 were estimated to be 30,000, 2,800, and 210,000 M^{-1} for Cl^-, Br^-, and $CH_3CO_2^-$, respectively [33].

In the solid state, a series of anion receptors may assemble in various assembling modes in the forms of receptor–anion complexes by combination with counter cations. *β*-Unsubstituted **1b** afforded a planar [1 + 1]-type pentacoordinated Cl^- complex **1b**·Cl^- that involved the pyrrole NH, the bridging CH, and phenyl *ortho*-CH units (Fig. 9.3a). Planar anion **1b**·Cl^- stacked with tetrapropylammonium cations (TPA^+) to form a charge-by-charge columnar structure with a Cl···Cl distance of 8.54 Å, and a separation of 7.29 Å between the **1b**·Cl^- units

(Fig. 9.3a(i)) [33]. Similarly, β-substituted **2b** and **3b** formed [1 + 1]-type complexes **2b**·Cl^- and **3b**·Cl^-; they assembled into columnar structures with the counter cations, with the TPA^+ salt of **2b**·Cl^- showing alternately stacking cationic and anionic components and the TBA^+ salt of **3b**·Cl^- forming a columnar assembly of two **3b**·Cl^- and two TBA^+ in a row (Fig. 9.3b(i), c(i)) [39]. The effects of the cation geometries were observed in the case of the planar 4,8,12-tripropyl-4,8,12-triazatriangulenium cation ($TATA^+$) [49, 50] in place of the tetraalkylammonium cations. In fact, like **1b**·Cl^--TPA^+, the ion pair **1b**·Cl^--$TATA^+$ formed a charge-by-charge columnar structure, but with a smaller distance between the **1b**·Cl^- units (6.85 and 7.29 Å for $TATA^+$ and TPA^+ salts, respectively) (Fig. 9.3a(ii)) [37]. Furthermore, both β-methyl **2b**·Cl^--$TATA^+$ and β-fluorinated **3b**·Cl^--$TATA^+$ also formed columnar assemblies with alternately stacking receptor–Cl^- complexes and $TATA^+$ cations (Fig. 9.3b(ii), c(ii)). It is noteworthy that the Cl···Cl distances of 12.43 and 10.57 Å for **2b**·Cl^--$TATA^+$ and **3b**·Cl^--$TATA^+$, respectively, along the columns were much longer than the 6.85 Å observed for **1b**·Cl^--$TATA^+$. As related to this observation, the smaller overlaps between the receptor–Cl^- complexes and $TATA^+$ in **2b**·Cl^--$TATA^+$ and **3b**·Cl^--$TATA^+$ implied that the β-substituents of the receptor molecules may interfere with the formation of stable charge-by-charge columnar structures [42].

9.3 Thermotropic Liquid Crystals Based on Planar Receptor–Anion Complexes and Appropriate Cations

Modification at the periphery of anion receptor molecules makes it possible to form dimension-controlled organized structures as liquid crystals. In particular, introduction of aliphatic chains to π-conjugated molecules, as seen for **1c**, **2c**, and **3c** (Fig. 9.4a), is an effective strategy for fabricating such assemblies. For example, **1c** appeared as a thermotropic liquid crystal with a mesophase at 36.7–172.5 °C, as revealed by differential scanning calorimetry (DSC). Polarized optical microscopy (POM) showed a ribbon-like texture, and X-ray diffraction (XRD) measurement suggested the formation of a hexagonal columnar (Col_h) phase, in which one unit lattice consisted of a dimer ($Z = 2$ for $\rho = 1$, $a = 3.98$ nm for **1c**) (Fig. 9.4b(i)). Although it is rare to form a stacking columnar structure comprising two rod-like molecules, it can be achieved by N–H···F–B hydrogen-bonding and dipole–dipole interactions. Flash-photolysis time-resolved microwave conductivity (FP-TRMC) measurement [51–54] demonstrated crystal-state charge-carrier mobility in **1c** (0.25 $cm^2\ V^{-1}\ s^{-1}$) at 25 °C, suggesting that **1c** may be useful as an electrically conductive material [35]. Furthermore, β-methyl **2c** and β-fluorinated **3c** showed similar Col_h mesophases ($a = 4.30$ and 4.18 nm, respectively) with transition temperatures (°C) of 89/44 (1st cooling) and 32/101 (2nd heating) for **2c** and 202/42 (1st cooling) and 45/204 (2nd heating) for **3c** (Fig. 9.4b(ii, iii)) [42].

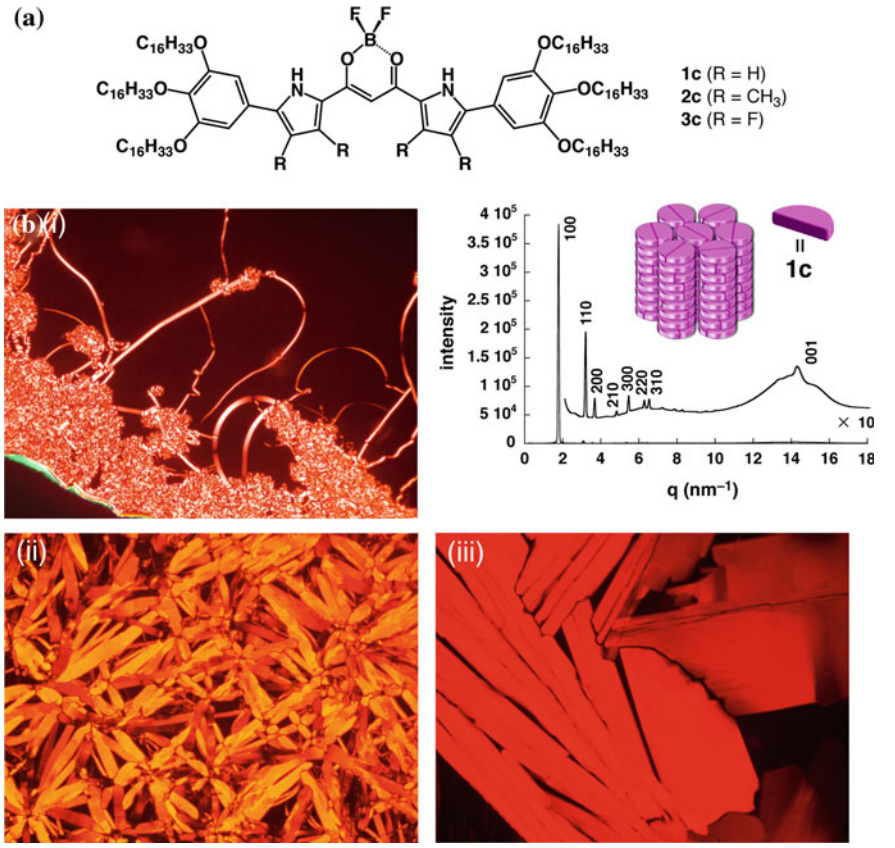

Fig. 9.4 **a** Anion receptors possessing long alkyl chains and **b** POM images of *i* **1c**, *ii* **2c**, and *iii* **3c** as mesophases at 170, 70, and 196 °C, respectively, upon cooling from Iso. Also shown in **b***i* is the synchrotron XRD pattern of **1c** at 120 °C upon cooling from Iso and a proposed Col_h model. The XRD by synchrotron irradiation was performed in [42] and the data was basically consistent with the XRD in [35]

Mesophase behaviors were also observed in ion-based assemblies of **1c**, **2c**, and **3c** as $TATA^+$ salts of receptor–Cl^- complexes. DSC analysis of **1c**·Cl^--$TATA^+$ suggested the formation of a mesophase, as observed in the phase transitions at 88/42 °C (1st cooling) and at 44/96 °C (2nd heating). Cooling from the isotropic liquid (Iso) afforded larger focal conic domains and dark domains in the POM images (Fig. 9.5a(i)), suggesting that discotic columnar structures were well aligned perpendicularly to the substrates. Upon cooling to 70 °C from Iso, synchrotron XRD analysis showed the relatively sharp peaks of a Col_h phase with $a = 4.64$ nm and $c = 0.73$ nm based on a tetrameric assembly ($Z = 3.58$ for $\rho = 1$) (Fig. 9.5a(ii)), with shear-driven alignment of the columnar structure. The c value of 0.73 nm corresponded to the distance ascribed to the alternately stacking ion pairs of **1c**·Cl^- and $TATA^+$, strongly suggesting the contribution of a

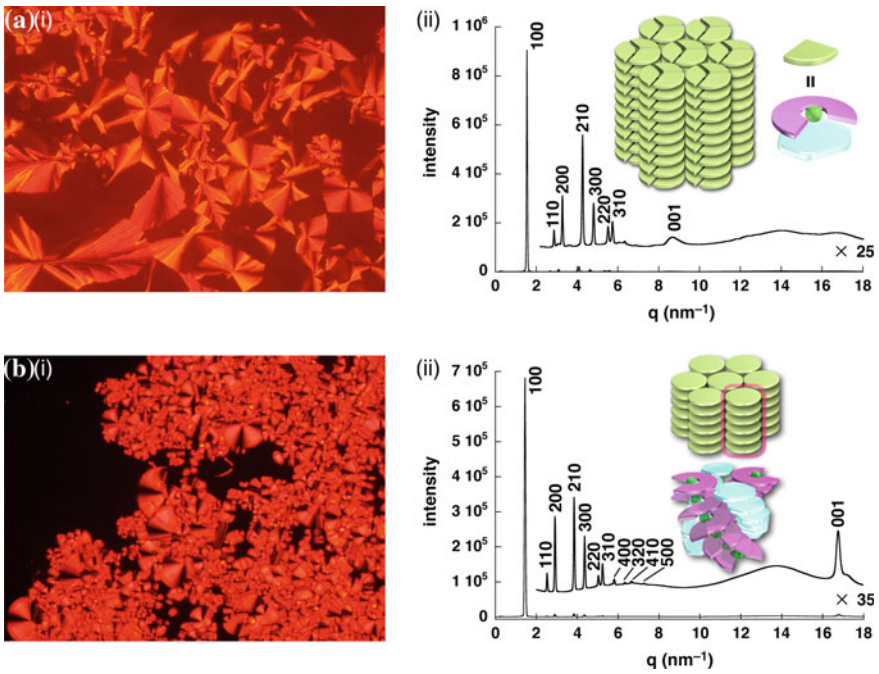

Fig. 9.5 *i* POM images and *ii* synchrotron XRD patterns of (**a**) **1c**·Cl^--$TATA^+$ (70 °C for both cases) and (**b**) **2c**·Cl^--$TATA^+$ (150 and 101 °C, respectively) upon cooling from Iso along with proposed Col_h models based on charge-by-charge and charge-segregated assemblies

charge-by-charge assembly, whereas the circular tetrameric assembly in a single disk unit was also consistent with the fan-like geometry of **1c**·Cl^-. As a preliminary result, the application of an electric field in the mesophase resulted in an optical response, as observed in the POM images [37]. On the other hand, **2c**·Cl^--$TATA^+$ and **3c**·Cl^--$TATA^+$ exhibited POM textures as mesophases (Fig. 9.5b(i)), with transition temperatures (°C) of 149/34 (1st cooling) and 40/153 (2nd heating) and 145/38 (1st cooling) and 45/146 (2nd heating), respectively. Synchrotron XRD analysis of the mesophases of **2c**·Cl^--$TATA^+$ and **3c**·Cl^--$TATA^+$ revealed Col_h structures with $a = 4.99$ nm and $c = 0.37$ nm ($Z = 2.05$ for $\rho = 1$) and $a = 4.92$ nm and $c = 0.37$ nm ($Z = 1.98$ for $\rho = 1$), respectively (Fig. 9.5b(ii)). The periodicity of 0.37 nm comparable to the ordinary π–π stacking distances strongly suggested the local stacking of identically charged planes. The contribution of the charge-segregated assembly may result from the distorted π-conjugated units owing to the β-substituents [42].

Time-of-flight (TOF) electrical conductivity measurements of ion-based materials **1c**·Cl^--$TATA^+$, **2c**·Cl^--$TATA^+$, and **3c**·Cl^--$TATA^+$ indicated ambipolar charge-carrier transport behavior with well-balanced values at high mobilities (10^{-2}–10^{-3} $cm^2\ V^{-1}\ s^{-1}$) for both holes and electrons without special purification procedures. The highest value of the zero-field limit mobility was observed for the

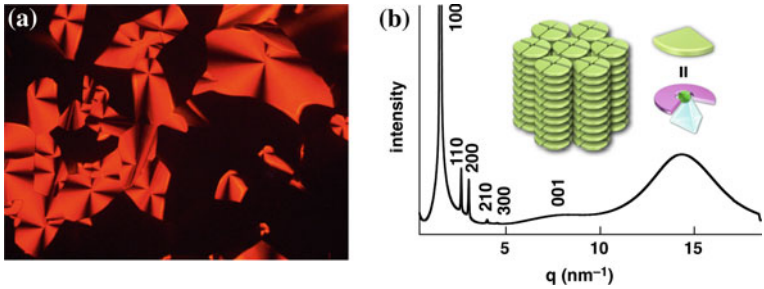

Fig. 9.6 **a** POM texture and **b** synchrotron XRD pattern of **1c**·Cl^--TBA^+ at 62 °C upon cooling from Iso and a proposed Col_h model based on charge-by-charge assembly

positive charge in **3c**·Cl^--$TATA^+$ (0.11 $cm^2\ V^{-1}\ s^{-1}$) probably as a result of the partial contribution of the charge-segregated assembly with distinct arrays of identical charged species. In the case of the negative charge carriers, **3c**·Cl^--$TATA^+$ exhibited almost equivalent values of mobility (5×10^{-3} $cm^2\ V^{-1}\ s^{-1}$ at $E = 4 \times 10^3$ V cm^{-1}) at 100–140 °C, with negligible electric-field dependence. The electron-deficient nature of **3c**·Cl^--$TATA^+$ led to higher stability of the electrons in the Col_h structure, resulting in relatively higher values of electron mobility [42]. Considering the results from these aliphatic receptors, the properties and packing structures of ion-based assemblies can be modulated by further modifications of the anion receptors, such as semifluoroalkyl-substituted [46], β-benzo- and β-corannulene-fused [41, 45], and boron-modified derivatives [44].

Not only planar cations, but bulky cations can also act as building blocks for the formation of ion-based assemblies, even though their steric hindrance interferes with the stacking of the receptor–anion complexes. Similar to the assemblies of planar cations, Col_h mesophases based on charge-by-charge assembly were obtained by the complexation of **1c** with Cl^- as the salts of different tetraalkylammonium cations $n_mMe_{4-m}N^+$ ($(C_nH_{2n+1})_mMe_{4-m}N^+$: $m = 1$–4) (Table 9.1), with broken-fan-like POM textures seen upon cooling from Iso (Fig. 9.6a for **1c**·Cl^--TBA^+ (4_4N^+)). In this case, **1c**·Cl^--TBA^+ as a Col_h mesophase included alternately stacking planar **1c**·Cl^- and bulky TBA^+ via charge-by-charge assembly (Fig. 9.6b). As seen in Table 9.1, ion pairs of a planar anionic component and a bulky tetraalkylammonium cation tune their assembled structures and properties according to the number and length of the aliphatic chains in the employed cations. In particular, as the chain number and length increased, the ability of the cations to assemble with **1c**·Cl^- was reduced owing to the increased steric hindrance, resulting in the formation of ionic liquids at fairly low temperatures [40].

Cationic species as counterparts of the planar receptor–anion complexes can be prepared by *anion binding*. In fact, organized structures based on planar charged species were fabricated by combining positively and negatively charged receptor–anion complexes using dicationic and electronically neutral π-conjugated receptors. Phenylene- or pyrimidine-bridged bis(imidazolium) dicationic anion receptors

Table 9.1 Phase transitions of **1c**·Cl^--$n_m$$Me_{4-m}N^+$

1c·Cl^--$n_m$$Me_{4-m}N^+$		Cooling[a]	Heating[a]
1c·Cl^--$n_1Me_3N^+$	$n = 8$	Cr[c] 36.3 Col_h 72.1 Iso	Cr[c] 43.3 Col_h 74.5 Iso
	$n = 12$	Cr[c] 37.9 Col_h 72.3 Iso	Cr[c] 42.9 Col_h 73.8 Iso
	$n = 16$	Cr[c] 41.9 Col_h 68.1 Iso	Cr[c] 44.9 Col_h 73.0 Iso
1c·Cl^--$n_2Me_2N^+$	$n = 8$	Cr[c] 33.7 Col_h 61.2 Iso	Cr[c] 39.2 Col_h 62.6 Iso
	$n = 12$	Cr[c] 28.9 Col_h 69.1 Iso	Cr[c] 35.5 Col_h 70.1 Iso
	$n = 18$[b]	Cr[c] 40.2 Col_h 79.8 Iso	Cr[c] 44.5 Col_h 80.8 Iso
1c·Cl^--$n_3Me_1N^+$	$n = 4$	Cr[c] 41.9 Col_h 54.1 Iso	Cr[c] 46.2 Col_h 61.9 Iso
	$n = 8$	Cr[d] 30.5 Iso	Cr[d] 35.4 Iso
	$n = 12$	Cr[d] 24.5 Iso	Cr[d] 30.8 Iso
1c·Cl^--n_4N^+	$n = 4$	Cr[c] 40.3 Col_h 84.1 Iso	Cr[c] 46.5 Col_h 84.4 Iso
	$n = 8$	Cr[d] 29.2 Iso	Cr[d] 32.7 Cr′[e] 45.6 Iso
	$n = 12$	Cr[d] 23.6 Iso	Cr[d] 27.6 Cr′[e] 42.0 Iso

[a] Transition temperatures (°C, the onset of the peak) from DSC 1st cooling and 2nd heating scans (5 °C min^{-1})
[b] Used because 16_2Me_2NCl is not readily available
[c] Cr with Col_h structures
[d] Cr with unidentified structures
[e] Cr′ with rectangular columnar (Col_r) structures

4a^{2+}–**c**$^{2+}$ (Fig. 9.7a) [55, 56] as precursor cationic anion complexes formed monocationic receptor–Cl^- complexes that were accompanied by a free Cl^-. This free Cl^- was subsequently captured by electronically neutral anion receptors **1a–c** to form negatively charged receptor–Cl^- complexes. The ion pairs of the resulting positively and negatively charged planar receptor–Cl^- complexes showed mesophase behaviors. Typical POM textures such as broken-fan-shaped types were observed during heating and cooling processes (Fig. 9.7b(i) for **1c**·Cl^--**4b**$^{2+}$·Cl^-). The phase transition temperatures (°C) of the ion pairs with **1c**·Cl^- were as 103.9/46.7 (**1c**·Cl^--**4a**$^{2+}$·Cl^-), 148.3/33.9 (**1c**·Cl^--**4b**$^{2+}$·Cl^-), and 119.3/28.8 (**1c**·Cl^--**4c**$^{2+}$·Cl^-) upon cooling from Iso. The temperature range of the mesophase in **1c**·Cl^--**4b**$^{2+}$·Cl^- was greater than that in **1c**·Cl^--**4a**$^{2+}$·Cl^- by incorporation of the pyrimidine moieties. The synchrotron XRD pattern of **1c**·Cl^--**4b**$^{2+}$·Cl^- at 115 °C showed the formation of a Col_h mesophase with $a = 4.34$ nm (Fig. 9.7b(ii)). Besides the sharp in-plane diffractions, a broad and weak peak appeared around 0.75 nm, which was derived from the stacking periodicity between the adjacent assembled units with the contribution of charge-by-charge assembly. After cooling to 20 °C, the Col_h structure was maintained, giving $a = 4.73$ nm, and the peak at 0.75 nm became more evident. Accordingly, the average number of ion pairs in an assembled unit (Z) was estimated to be 3 for $\rho = 1$ ($Z = 2.9$ and 3.4 at 115 and 20 °C, respectively). Meanwhile, **1c**·Cl^--**4a**$^{2+}$·Cl^- also provided a Col_h structure ($a = 4.65$ nm, $c = 0.75$ nm, and $Z = 3.3$ for $\rho = 1$ at 80 °C upon cooling from Iso), whereas **1c**·Cl^--**4c**$^{2+}$·Cl^- had complicated XRD patterns, which may be ascribed to the increased rigidity of the dicationic anion receptor with the introduction of aryl moieties. The observations by synchrotron XRD indicated that the

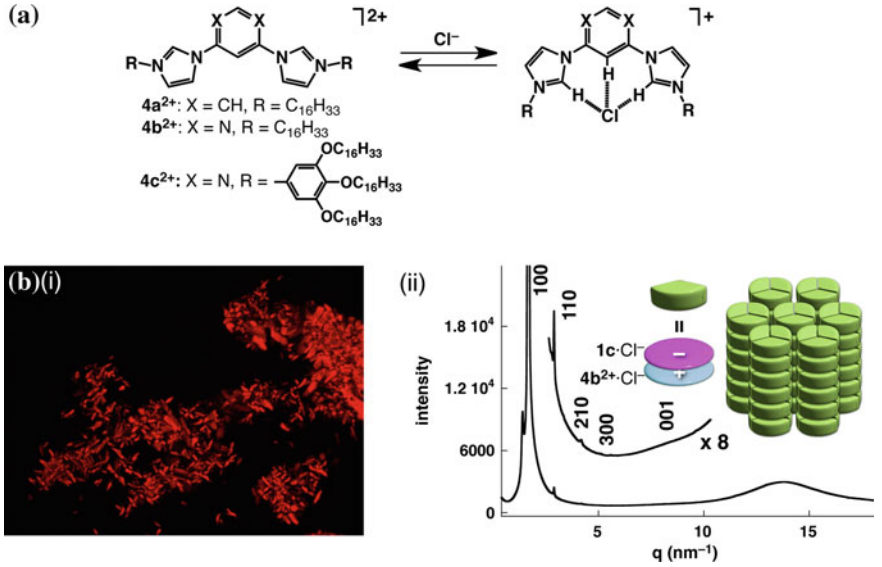

Fig. 9.7 **a** Positively charged anion receptors and their Cl^--binding modes forming cationic receptor–Cl^- complexes and **b***i* POM texture and *ii* synchrotron XRD pattern of **1c**·Cl^--**4b**$^{2+}$·Cl^- at 115 °C upon cooling from Iso, along with a proposed Col_h model wherein the exact molecular orientation cannot be shown

introduction of dicationic anion receptors was effective for constructing ordered assembled structures. It is noteworthy that the geometries in the core π-conjugated parts of the cationic and anionic receptor–Cl^- complexes are quite similar by considering the constituents, one six-membered ring at the center and two neighboring five-membered rings. The similarity in the sizes and shapes of the two ionic components is a very important factor in forming assemblies consisting of multiple components. Furthermore, using the FP-TRMC technique, the one-dimensional charge-carrier transporting properties, with the mobilities of 0.05 and 0.03 $cm^2\ V^{-1}\ s^{-1}$ for **1c**·Cl^--**4a**$^{2+}$·Cl^- and **1c**·Cl^--**4b**$^{2+}$·Cl^-, respectively, were observed for the newly prepared solid-state ion pairs [48].

In the preceding examples, the dimension-controlled organized structures in the ion-based materials were mainly fabricated by van der Waals interactions between the aliphatic chains of the receptor molecules. In contrast, the anion receptors in the absence of aliphatic chains were found to form dimension-controlled structures by combination with cationic species possessing aliphatic units. In fact, the employment of benzyltrialkylammonium chlorides (16Bn_3NCl, $n = 2$ and 4) and benzylpyridinium chloride (16BPyCl) (Fig. 9.8a) with β-unsubstituted **1a**, **b** and β-fluorinated **3a**, **b** resulted in the construction of ion-based assemblies. Cl^- complexes of **1a**, **b** and **3a**, **b** as 16Bn_3N$^+$ ($n = 2$ and 4) and 16BPy$^+$ salts showed different thermal behaviors from the individual components (Table 9.2). Self-organization into mesophases was achieved by the delicate balance between the

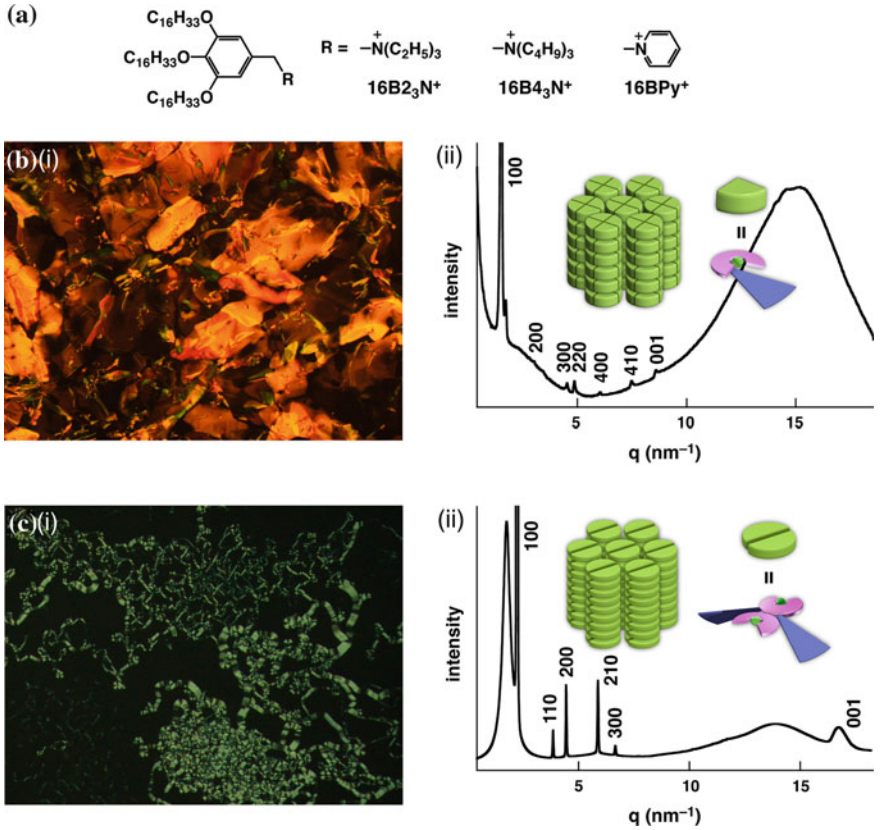

Fig. 9.8 **a** Structures of 16Bn_3NCl (n = 2 and 4) and 16BPyCl; *i* POM textures and *ii* synchrotron XRD patterns of **b** **1b**·Cl^--16B4_3N^+ (125 and 90 °C, respectively) and **c** **3a**·Cl^--16B2_3N^+ (85 °C for both cases) upon 2nd heating, along with proposed Col_h models, wherein module cations are shown as fan-like shapes based on the optimized structures and the charge-by-charge and charge-segregated assemblies are represented by thick and thin disk components, respectively

positively and negatively charged components, in terms of the size of the ionic parts in the cation species and the substituents on the anion receptors. For example, **1b**·Cl^--16B4_3N^+ and **3a**·Cl^--16B2_3N^+ showed flake-like and fiber-like POM textures, respectively, upon 2nd heating (Fig. 9.8b, c(i)), with the formation of Col_h mesophases with $a = 4.79$ and 3.28 nm and $c = 0.74$ and 0.38 nm, respectively (Fig. 9.8b, c(ii)). The c values of **1b**·Cl^--16B4_3N^+ and **3a**·Cl^--16B2_3N^+ indicated a charge-by-charge arrangement and the local stacking of identically charged species to produce a column, respectively. The β-substituents of the anion receptor, inductively electron-withdrawing fluorine moieties, were responsible for the contribution of the charge-segregated assembly, making the intermolecular interactions among the anionic complexes sufficiently robust for stacking structure formation. Furthermore, the charge-carrier mobilities $\sum\mu$ of

Table 9.2 Phase transitions[a] of cation-module Cl^- salts and their ion pairs in the presence of **1a**, **b** and **3a**, **b**

	$16B2_3NCl$	$16B4_3NCl$	16BPyCl
–	Cr^b 38.7 Cr'^b 63.7 Col_h 129.4[f] Iso	Cr^b 42.4 Cr'^c 54.0 Cr''^c 76.4 Iso [Cr^b 38.5 Col_h 81.0 Iso]	Cr^b 55.2 Cr'^b 81.1 Col_h 125.9[f] Iso
1a	Cr^b 50.1 Col_h 132.5[f] Iso	Cr^d 43.8 Iso	Cr^b 54.3 Col_h 133.7[f] Iso
1b	Cr^c 37.1 Cr'^c 45.6 Iso [Cr^c 40.4 Iso]	Cr^b 38.6 Col_h 143.1[f] Iso	Cr^c 48.3 Cr'^c 127.3[f] Iso
3a	Cr^c 6.5 Cr'^b 35.7 Col_h 102.4 Iso	Cr^b 39.1 Cr'^b 59.6 Cr''^b 92.1 Iso	Cr^b 39.3 Col_h 53.1[f] Iso
3b	Cr^e 29.1 Cr'^e 51.3 Iso [Cr^e 30.7 Cr'^e 49.4 Cr''^e 54.1 Iso]	Cr^d 30.7 M^e 69.8 Iso [Cr^d 36.6 M'^c 74.2 Iso]	Cr^b 30.2 Cr'^b 45.7 Iso

[a] Transition temperatures (°C, the onset of the peak) from DSC upon 2nd heating (5 °C min^{-1}). The entries in brackets show the transitions upon 1st cooling which exhibit phases different from those upon 2nd heating
[b] Basically as Col_h structures
[c] Unidentified structures
[d] Basically as lamellar structures
[e] Basically as Col_r structures
[f] Values from POM measurements

1b·Cl^--$16B4_3N^+$ and **3a**·Cl^--$16B2_3N^+$ were estimated by FP-TRMC measurements as 0.05 ± 0.01 and 0.22 ± 0.03 $cm^2\ V^{-1}\ s^{-1}$, respectively. The increase in mobility for the assembly with the contribution of the charge-segregated mode offers the possibility of enhanced efficiency of charge-carrier transport in organic electronic devices [43].

Anion receptors that cannot form soft materials by themselves can also form dimension-controlled organized structures by combining with anionic species possessing aliphatic units. The combination of **1a**, **b** with aliphatic-chain-substituted gallic carboxylates ($Ar^{Cn}CO_2^-$, n = 16, 18, and 20, Fig. 9.9a) as TBA^+ salts provided mesophases mainly of lamellar structures, with transition temperatures of 42/56/103, 67/73/101, and 67/81/96 °C for **1a**·$Ar^{Cn}CO_2^-$·TBA (n = 16, 18, and 20, respectively) and 40/61/81, 53/64/86, and 61/82/89 °C for **1b**·$Ar^{Cn}CO_2^-$·TBA (n = 16, 18, and 20, respectively) upon 2nd heating (Fig. 9.9b, c). The diffractions assignable to the charge-by-charge assemblies of receptor–carboxylate moieties and TBA^+ cations could not all be clearly observed, suggesting that fairly disordered structures were produced. On consideration of the crystal-state assembled mode of **1a**·$Ar^{C1}CO_2^-$-TPA^+, the modified anions may be located at distorted angles to the receptor planes and could predominantly control the assembled structures through van der Waals interactions between the aliphatic chains. Furthermore, on increasing the temperature from 28 to 67 °C, the electrical conductivity of **1b**·$Ar^{C16}CO_2^-$-TBA^+ increased from 5×10^{-11} to 3×10^{-8} S m^{-1}, owing to the increased population of thermally activated charge carriers with equivalent mobility in the mesophases. On the other hand, at r.t. upon cooling from

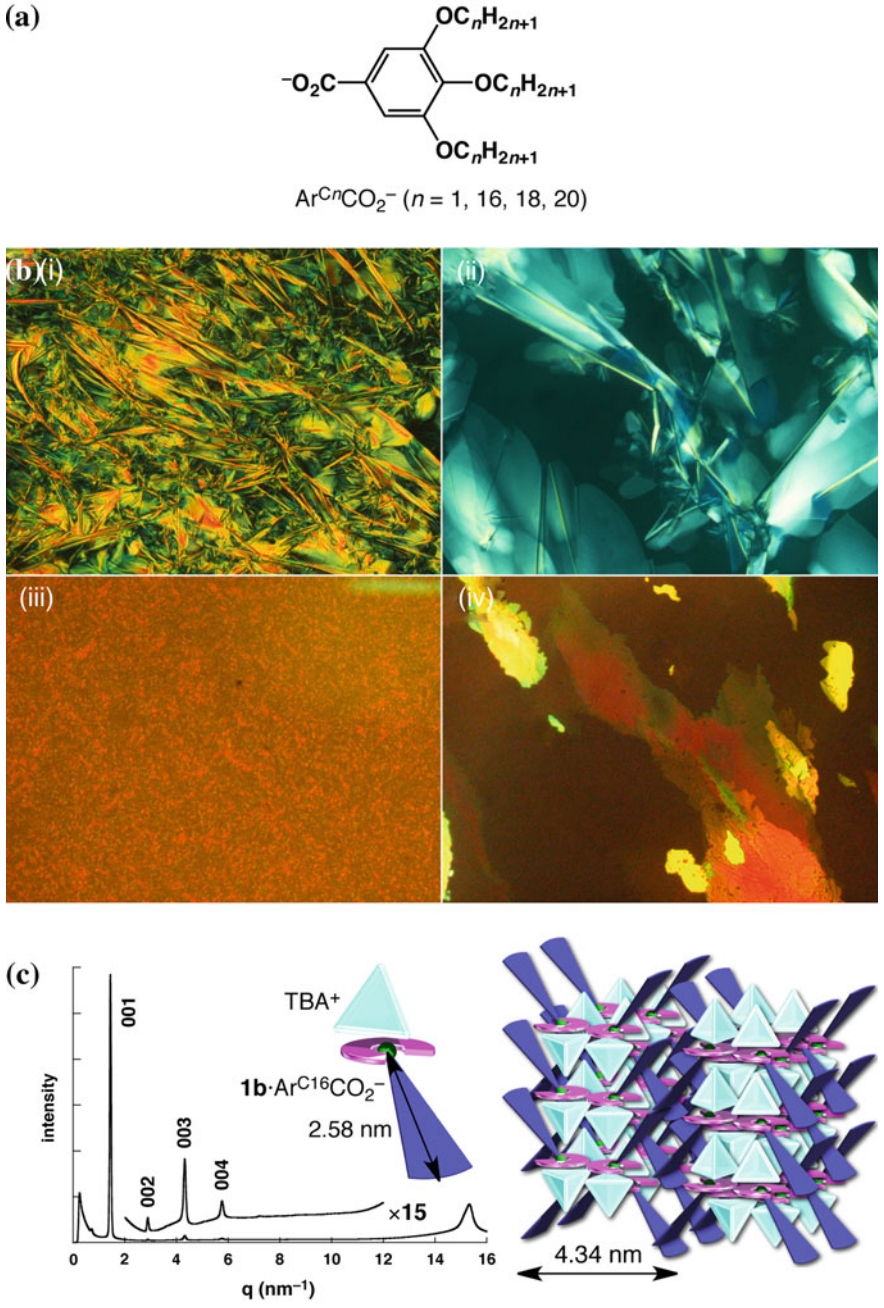

Fig. 9.9 **a** Structures of gallic carboxylates $Ar^{Cn}CO_2^-$ (n = 1, 16, 18, 20); **b** POM images of *i* **1a**·$Ar^{C18}CO_2^-$-TBA^+ at 95 °C, *ii* **1a**·$Ar^{C20}CO_2^-$-TBA^+ at 92 and 80 °C, *iii* **1b**·$Ar^{C16}CO_2^-$-TBA^+ at 80.5 °C, and *iv* **1b**·$Ar^{C18}CO_2^-$-TBA^+ at 83 °C upon cooling from Iso; **c** synchrotron XRD pattern (*left*) and a proposed assembled model (*right*) of **1b**·$Ar^{C16}CO_2^-$-TBA^+ as the solid state at r.t. upon cooling from Iso, suggesting that the observed assembled structure was more disordered than the proposed model, with a value of 2.58 nm estimated by density functional theory (DFT) calculations

Iso, **1a**·$Ar^{C16}CO_2^-$-TBA^+ and **1b**·$Ar^{C16}CO_2^-$-TBA^+ showed charge-carrier mobilities of 0.02 and 0.05 $cm^2\ V^{-1}\ s^{-1}$, respectively. At elevated temperatures, the values for **1a**·$Ar^{C16}CO_2^-$-TBA^+ decreased to 0.007 and 9×10^{-4} $cm^2\ V^{-1}\ s^{-1}$ at 46 and 70 °C, respectively, whereas those for **1b**·$Ar^{C16}CO_2^-$-TBA^+ were 0.003 and 0.04 $cm^2\ V^{-1}\ s^{-1}$ at 50 and 70 °C, respectively, owing to transitions between the solid state and different mesophases [38].

9.4 Thermotropic Liquid Crystals Based on Planar Ion Pairs

The choice of constituent anion-responsive π-conjugated molecules is very important for controlling the assembly modes of ion-based organized structures. As a building subunit of the π-conjugated molecules, pyrazole can interact electrostatically or via hydrogen bonding with anionic or polar substrates in its partially or fully protonated form. Dipyrrolylpyrazoles (DPPs) (**5a–c** and **6a–c**, Fig. 9.10a(i)), which are small simple structures, are potential candidate precursors for positively charged π-electronic units as they form planar [2 + 2]-type complexes in their protonated forms by combination with trifluoroacetate ($CF_3CO_2^-$) (Fig. 9.10a(i)) [57, 58]. The [2 + 2]-type complexes of **5a**·H^+ and **6a**·H^+ with $CF_3CO_2^-$ formed herringbone-like stacking assemblies in the solid state (Fig. 9.10b) [57]. Based on these observations, it was deduced that an appropriate arrangement of [2 + 2]-type complexes of modified DPPs such as **5c** and **6c** could lead to ordered structures such as stacking columnar assemblies. Ion pairs **5c**·H^+ and **6c**·H^+ as $CF_3CO_2^-$ complexes exhibited enantiotropic mesophases at 66–85 °C (M1) and 85–96 °C (M2) (**5c**·H^+-$CF_3CO_2^-$) and at 68–131 °C (**6c**·H^+-$CF_3CO_2^-$) upon cooling from Iso. POM of **5c**·H^+ as a $CF_3CO_2^-$ complex showed a broken-fan-like texture and no texture for M1 and M2, respectively (Fig. 9.10c(i)), whereas **6c**·H^+-$CF_3CO_2^-$ as a mesophase exhibited a sand-like POM texture (Fig. 9.10d(i)). In contrast to **5c**, which showed no mesophase, **5c**·H^+-$CF_3CO_2^-$ as M2 at 90 °C upon cooling from Iso indicated the formation of a cubic (Cub) ($Pn\bar{3}m$) phase with $a = 10.9$ nm (Fig. 9.10c(ii)). **5c**·H^+-$CF_3CO_2^-$ as M1 at 80 °C showed a slightly complicated phase as a mixture of a rectangular columnar (Col_r) phase ($a = 7.32$ nm, $b = 3.52$ nm, and $Z =$ ca. 2 for $\rho = 1$) and another phase such as Cub. On the other hand, similar to **6c** showing a Col_h phase ($Z =$ ca. 2 for $\rho = 1$) with $a = 4.00$ nm (80 °C), **6c**·H^+-$CF_3CO_2^-$ as a mesophase indicated the formation of a Col_h phase ($a = 3.91$ nm at 120 °C) based on a [2 + 2]-type complex ($Z =$ ca. 2 for $\rho = 1$) (Fig. 9.10d(ii)). In this study, the anion ($CF_3CO_2^-$) served as a bridging unit connecting two cationic π-electronic species, resulting in the formation of a larger planar area as a subunit of the columnar structure [58].

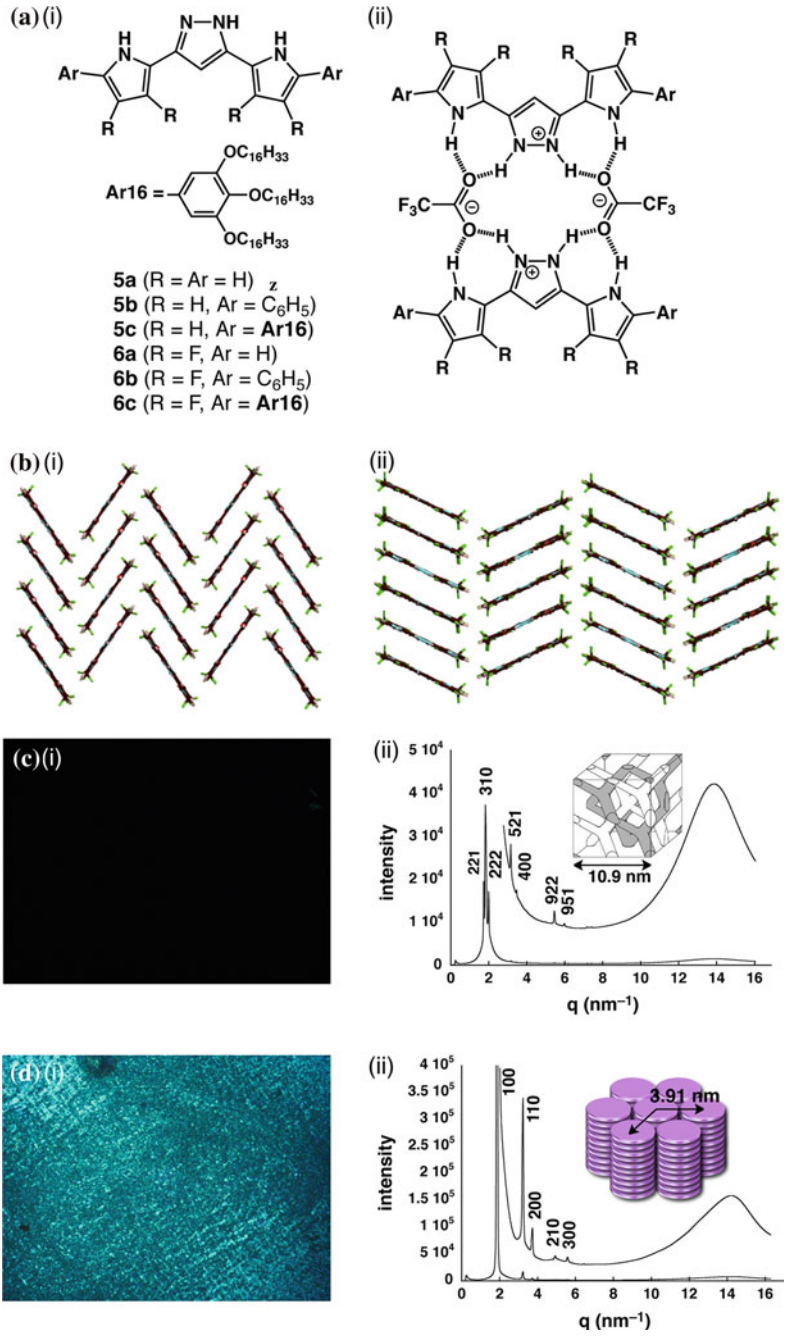

Fig. 9.10 **a** *i* Dipyrrolylpyrazoles (DPPs) and *ii* planar [2 + 2]-type complexes; **b** solid-state stacking diagrams of [2 + 2] assemblies of *i* $\mathbf{5a}_2{\cdot}TFA_2$ and *ii* $\mathbf{6a}_2{\cdot}TFA_2$ (reproduced from cif files: CCDC-625142, 625144); *i* POM images and *ii* synchrotron XRD patterns with proposed Cub and Col_h models (insets) of **c** $\mathbf{5c}{\cdot}H^+{-}CF_3CO_2^-$ and **d** $\mathbf{6c}{\cdot}H^+{-}CF_3CO_2^-$ as mesophases at 90 and 120 °C, respectively, upon cooling from Iso

9.5 Summary

This chapter discussed selected examples of ion-based thermotropic liquid crystals mainly comprising anion complexes of π-conjugated molecules and counter cations. The ordered arrangement of positively and negatively charged ionic species for the fabrication of liquid crystal materials requires their appropriate geometries, substituents, and electronic properties. Among the candidate components for achieving such materials, the pyrrole-based anion receptors synthesized by our group have been demonstrated to be efficient motifs for the formation of planar anionic complexes by binding anions, resulting in the formation of supramolecular assemblies by combination with cationic species. Modification of the anion receptors and the appropriate choice of anions and cations were found to be effective in forming functional ion-based materials with contributions from charge-by-charge and charge-segregated modes. As demonstrated in this chapter, a variety of ion-based liquid crystal materials have been fabricated to date; however, the exact mechanisms of assembly have not yet been fully elucidated. The innovative design and synthesis of π-electronic systems by considering their geometries, electronic properties, and stabilities would enable the preparation of fascinating ion-based materials for use in improved electronic devices.

Acknowledgments The contributions reported herein have been supported by PRESTO, Japan Science and Technology Agency (JST) ("Structure Control and Function", 2007–2011), Grants-in-Aid for Young Scientists (B) (No. 21750155) and (A) (No. 23685032) and Scientific Research in a Priority Area "Super-Hierarchical Structures" (No. 18039038, 19022036) from the Ministry of Education, Culture, Sports, Science, and Technology (MEXT), the matching fund subsidies for private universities from the MEXT, 2003–2008 and 2009–2014, and the Ritsumeikan Global Innovation Research Organization (R-GIRO) project, 2008–2013. The author thanks all the authors and the collaborators described in the acknowledgement in the previous publications, in particular, Prof. Atsuhiro Osuka and his group members for single-crystal X-ray analysis, Dr. Takashi Nakanishi, NIMS, for his kind help with various analyses of molecular assemblies, Prof. Shu Seki, Osaka University, and his group members for electrical conductivity measurements, Prof. Hitoshi Tamiaki, Ritsumeikan University, for various measurements, and all the group members, especially, Dr. Yohei Haketa and Dr. Bin Dong, for their contributions on ion-based materials.

References

1. G. Tsoucaris (ed.), *Current Challenges on Large Supramolecular Assemblies, NATO Science Series* (Kluwer, South Holland, 1999)
2. A. Ciferri (ed.), *Supramolecular Polymers* (Marcel Dekker, New York, 2000)
3. F. Würthner (ed.), *Supramolecular Dye Chemistry*, *Topics in Current Chemistry*, vol. 258 (Springer, Berlin, 2005), pp. 1–324
4. J.L. Atwood, J.W. Steed (eds.), *Organic Nanostructures* (Wiley, Weinheim, 2007)
5. P.A. Gale, J.W. Steed (eds.), *Supramolecular Chemistry: From Molecules to Nanomaterials* (Jon Wiley & Sons, Chichester, 2012)
6. W. Hamley, *Introduction to Soft Matter—Polymers, Colloids, Amphiphiles and Liquid Crystals* (John Wiley & Sons, West Sussex, 2000)

7. I. Dierking, *Textures of Liquid Crystals* (Wiley, Weinheim, 2003)
8. T. Kato, N. Mizoshita, K. Kishimoto, Functional liquid-crystalline assemblies: self-organized soft materials. Angew. Chem. Int. Ed. **45**, 38–68 (2006)
9. T. Kato (ed.), *Liquid Crystalline Functional Assemblies and Their Supramolecular Structures, Structure and Bonding*, vol. 128 (Springer, Berlin, 2008), pp. 1–237
10. T. Kato, T. Yasuda, Y. Kamikawa, M. Yoshio, Self-assembly of functional columnar liquid crystals. Chem. Commun. **12**, 729–739 (2009)
11. B.R. Kaafarani, Discotic liquid crystals for opto-electronic applications. Chem. Mater. **23**, 378–396 (2011)
12. S. Kumar, *Chemistry of Discotic Liquid Crystals: From Monomers to Polymers; The Liquid Crystals Book Series* (CRC Press, Boca Raton, 2011)
13. T. Welton, Room-temperature ionic liquids. solvents for synthesis and catalysis. Chem. Rev. **99**, 2071–2084 (1999)
14. P. Wasserscheid, W. Keim, Ionic liquids—new solutions for transition metal catalysis. Angew. Chem. Int. Ed. **39**, 3772–3789 (2000)
15. H. Ohno, Functional design of ionic liquids. Bull. Chem. Soc. Jpn. **79**, 1665–1680 (2006)
16. M.A.P. Martins, C.P. Frizzo, D.N. Moreira, N. Zanatta, H.G. Bonacorso, Ionic liquids in heterocyclic synthesis. Chem. Rev. **108**, 2015–2050 (2008)
17. P. Hapiot, C. Lagrost, Electrochemical reactivity in room-temperature ionic liquids. Chem. Rev. **108**, 2238–2264 (2008)
18. R. Giernoth, Task-specific ionic liquids. Angew. Chem. Int. Ed. **49**, 2834–2839 (2010)
19. K. Binnemans, Ionic liquid crystals. Chem. Rev. **105**, 4148–4204 (2005)
20. T.L. Greaves, F.J. Drummond, Ionic liquids as amphiphile self-assembly media. Chem. Soc. Rev. **37**, 1709–1726 (2008)
21. K.V. Axenov, S. Laschat, Thermotropic ionic liquid crystals. Materials **4**, 206–259 (2011)
22. A. Bianchi, K. Bowman-James, E. García-España (eds.), *Supramolecular Chemistry of Anion* (Wiley, New York, 1997)
23. R.P. Singh, B.A. Moyer (eds.), *Fundamentals and Applications of Anion Separation* (Kluwer, New York, 2004)
24. I. Stibor (ed.), *Anion Sensing*, *Topics in Current Chemistry*, vol. 255 (Springer, Berlin, 2005), pp. 1–238
25. J.L. Sessler, P.A. Gale, W.-S. Cho, *Anion Receptor Chemistry* (RSC, UK, 2006)
26. R. Vilar (ed.), *Recognition of Anions*, *Structure and Bonding*, vol. 129 (Springer, Berlin, 2008), pp. 1–252
27. P.A. Gale, W. Dehaen (eds.), *Anion Recognition by Supramolecular Chemistry, Topics in Heterocyclic Chemistry*, vol. 24 (Springer, Berlin, 2010), pp. 1–370
28. K. Bowman-James, A. Bianchi, E. García-España (eds.), *Anion Coordination Chemistry* (Wiley, Weinheim, 2011)
29. B. Dong, H. Maeda, Ion-based materials comprising planar charged species. Chem. Commun. **49**, 4085–4099 (2013)
30. H. Maeda, Y. Bando, Recent progress in research on anion-responsive pyrrole-based π-conjugated acyclic molecules. Chem. Commun. **49**, 4100–4113 (2013)
31. H. Maeda. Supramolecular chemistry of pyrrole-based π-conjugated molecules. Bull. Chem. Soc. Jpn. **86**, 1359–1399 (2013)
32. H. Maeda, Y. Kusunose, Dipyrrolyldiketone difluoroboron complexes: novel anion sensors with C-H$\cdots$X$^-$ interactions. Chem. Eur. J. **11**, 5661–5666 (2005)
33. H. Maeda, Y. Haketa, T. Nakanishi, Aryl-substituted C_3-bridged oligopyrroles as anion receptors for formation of supramolecular organogels. J. Am. Chem. Soc. **129**, 13661–13674 (2007)
34. H. Maeda, Y. Ito, Y. Haketa, N. Eifuku, E. Lee, M. Lee, T. Hashishin, K. Kaneko, Solvent-assisted organized structures based on amphiphilic anion-responsive π-conjugated systems. Chem. Eur. J. **15**, 3706–3719 (2009)

35. H. Maeda, Y. Terashima, Y. Haketa, A. Asano, Y. Honsho, S. Seki, M. Shimizu, H. Mukai, K. Ohta, Discotic columnar mesophases derived from 'rod-like' π-conjugated anion-responsive acyclic oligopyrroles. Chem. Commun. **46**, 4559–4561 (2010)
36. H. Maeda, Y. Bando, Y. Haketa, Y. Honsho, S. Seki, H. Nakajima, N. Tohnai, Electronic and optical properties in the solid-state molecular assemblies of anion-responsive pyrrole-based π-conjugated systems. Chem. Eur. J. **16**, 10994–11002 (2010)
37. Y. Haketa, S. Sasaki, N. Ohta, H. Masunaga, H. Ogawa, N. Mizuno, F. Araoka, H. Takezoe, H. Maeda, Oriented salts: dimension-controlled charge-by-charge assemblies from planar receptor–anion complexes. Angew. Chem. Int. Ed. **49**, 10079–10083 (2010)
38. H. Maeda, K. Naritani, Y. Honsho, S. Seki, Anion modules: building blocks of supramolecular assemblies by combination with π-conjugated anion receptors. J. Am. Chem. Soc. **133**, 8243–8896 (2011)
39. Y. Haketa, S. Sakamoto, K. Chigusa, T. Nakanishi, H. Maeda, Synthesis, crystal structures, and supramolecular assemblies of pyrrole-based anion receptors bearing modified pyrrole *β*-substituents. J. Org. Chem. **76**, 5177–5184 (2011)
40. B. Dong, Y. Terashima, Y. Haketa, H. Maeda, Charge-based assemblies comprising planar receptor–anion complexes with bulky alkylammonium cations. Chem. Eur. J. **18**, 3460–3463 (2012)
41. Y. Bando, S. Sakamoto, I. Yamada, Y. Haketa, H. Maeda, Charge-based and charge-free molecular assemblies comprising π-extended derivatives of anion-responsive acyclic oligopyrroles. Chem. Commun. **48**, 2301–2303 (2012)
42. Y. Haketa, Y. Honsho, S. Seki, H. Maeda, Ion materials comprising planar charged species. Chem. Eur. J. **18**, 7016–7020 (2012)
43. B. Dong, T. Sakurai, Y. Honsho, S. Seki, H. Maeda, Cation modules as building blocks forming supramolecular assemblies with planar receptor–anion complexes. J. Am. Chem. Soc. **135**, 1284–1287 (2013)
44. Y. Terashima, M. Takayama, K. Isozaki, H. Maeda, Ion-based materials of boron-modified dipyrrolyldiketones as anion receptors. Chem. Commun. **49**, 2506–2508 (2013)
45. Y. Bando, T. Sakurai, S. Seki, H. Maeda, Corannulene-fused anion-responsive π-conjugated molecules that form self-assemblies with unique electronic properties. Chem. Asian J. **8**, 2088–2095 (2013)
46. Y. Terashima, T. Sakurai, Y. Bando, S. Seki, H. Maeda, Assembled structures of anion-responsive π-systems tunable by alkyl/perfluoroalkyl segments in peripheral side chains. Chem. Mater. **25**, 2656–2662 (2013)
47. H. Maeda, W. Hane, Y. Bando, Y. Terashima, Y. Haketa, H. Shibaguchi, T. Kawai, M. Naito, K. Takaishi, M. Uchiyama, A. Muranaka, Chirality induction by formation of assembled structures based on anion-responsive π-conjugated molecules. Chem. Eur. J. **19**, 16263–16271 (2013)
48. B. Dong, T. Sakurai, Y. Bando, S. Seki, K. Takaishi, M. Uchiyama, A. Muranaka, H. Maeda, Ion-based materials derived from positively and negatively charged chloride complexes of π-conjugated molecules. J. Am. Chem. Soc. **135**, 14797–14805 (2013)
49. B.W. Laursen, F.C. Krebs, Synthesis of a triazatriangulenium salt. Angew. Chem. Int. Ed. **39**, 3432–3434 (2000)
50. B.W. Laursen, F.C. Krebs, Synthesis, structure, and properties of azatriangulenium salts. Chem. Eur. J. **7**, 1773–1783 (2001)
51. Y. Yamamoto, T. Fukushima, Y. Suna, N. Ishii, A. Saeki, S. Seki, S. Tagawa, M. Taniguchi, T. Kawai, T. Aida, Photoconductive coaxial nanotubes of molecularly connected electron donor and acceptor layers. Science **314**, 1761–1764 (2006)
52. A. Saeki, S. Seki, T. Sunagawa, K. Ushida, S. Tagawa, Charge-carrier dynamics in polythiophene films studied by in situ measurement of flash-photolysis time-resolved microwave conductivity (FP-TRMC) and transient optical spectroscopy (TOS). Philos. Mag. **86**, 1261–1276 (2006)

53. T. Umeyama, N. Tezuka, S. Seki, Y. Matano, M. Nishi, K. Hirao, H. Lehtivuori, V.N. Tkachenko, H. Lemmetyinen, Y. Nakao, S. Sakaki, H. Imahori, Selective formation and efficient photocurrent generation of [70]fullerene–single-walled carbon nanotube composites. Adv. Mater. **22**, 1767–1770 (2010)
54. Y. Yasutani, A. Saeki, T. Fukumatsu, T. Koizumi, S. Seki, Unprecedented high local charge-carrier mobility in P3HT revealed by direct and alternating current methods. Chem. Lett. **42**, 19–21 (2013)
55. K. Sato, S. Takeuchi, S. Arai, M. Yamaguchi, T. Yamagishi, 4, 6-Bis(imidazolio)pyrimidine as a new anion receptor. Heterocycles **73**, 209–215 (2007)
56. A. Rit, T. Pape, F.E. Hahn, Self-assembly of molecular cylinders from polycarbene ligands and Ag^{I} or Au^{I}. J. Am. Chem. Soc. **132**, 4572–4573 (2010)
57. H. Maeda, Y. Ito, Y. Kusunose, T. Nakanishi, Dipyrrolylpyrazoles: anion receptors in protonated form and efficient building blocks for organized structures. Chem. Commun. 1136–1138 (2007)
58. H. Maeda, K. Chigusa, T. Sakurai, K. Ohta, S. Uemura, S. Seki, Ion-pair-based assemblies comprising pyrrole–pyrazole hybrids. Chem. Eur. J. **19**, 9224–9233 (2013)